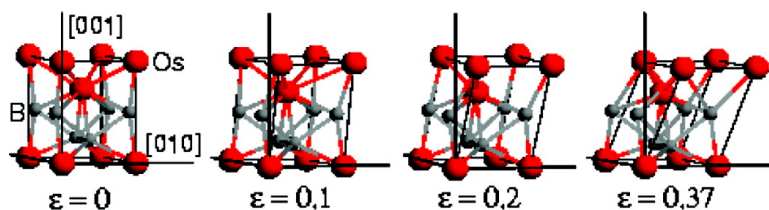


## Is Osmium Diboride An Ultra-Hard Material?

Jun Yang, Hong Sun, and Changfeng Chen

*J. Am. Chem. Soc.*, **2008**, 130 (23), 7200-7201 • DOI: 10.1021/ja801520v • Publication Date (Web): 14 May 2008

Downloaded from <http://pubs.acs.org> on February 8, 2009



### More About This Article

Additional resources and features associated with this article are available within the HTML version:

- Supporting Information
- Access to high resolution figures
- Links to articles and content related to this article
- Copyright permission to reproduce figures and/or text from this article

[View the Full Text HTML](#)

## Is Osmium Diboride An Ultra-Hard Material?

Jun Yang,<sup>†</sup> Hong Sun,<sup>\*,†</sup> and Changfeng Chen<sup>\*,‡</sup>

Department of Physics, Shanghai Jiao Tong University, Shanghai 200240, China, and Department of Physics and High Pressure Science and Engineering Center, University of Nevada, Las Vegas, Nevada 89154

Received February 28, 2008; E-mail: hsun@sjtu.edu.cn; chen@physics.unlv.edu

Developing new design principles for ultra-hard materials suitable for applications as abrasives and cutting tools for ferrous metals as well as scratch-resistance coatings is a research field with considerable fundamental interest and practical importance. All carbon-based hard materials, including diamond, react with oxygen and iron at moderately high temperature, thus preventing them from being used as cutting tools for steels. Recently, a new design principle is proposed to synthesize ultra-hard materials by combining small, light covalent elements with large, electron-rich transition metals.<sup>1,2</sup> The covalent elements form strong, directional covalent bonds with the transition metals, while the high density of valence electrons from transition metals prevents the structures from being squeezed together, both of which enhance the resistance of the structures against large inelastic deformations, leading to increased hardness. A primary example and among the first synthesized following this principle is OsB<sub>2</sub>, which has an expected (scratch) hardness over that of sapphire (20 GPa) based on the observation that the OsB<sub>2</sub> powder readily scratches a polished sapphire window<sup>1</sup> and a Vickers hardness of 30 GPa (on its (001) plane) by microhardness measurement.<sup>3</sup> Also, on the basis of this principle, IrN<sub>2</sub> and OsN<sub>2</sub> were synthesized,<sup>4</sup> followed recently by ReB<sub>2</sub> with an average hardness over 30 GPa.<sup>5</sup>

Recently, considerable efforts have been devoted to studies of this new class of ultra-hard materials, including TMB<sub>2</sub> (TM = Os, Re, Tc, Ru, Hf, Ta, W, Pt),<sup>6–11</sup> TMN<sub>2</sub> (TM = Os, Ir, Pt),<sup>3,12</sup> and OsO<sub>2</sub>.<sup>12,13</sup> Calculations show that OsB<sub>2</sub> has a bulk modulus over 300 GPa, close to those of diamond (bulk modulus = 440 GPa; hardness = ~100 GPa) and cubic BN (bulk modulus = 370 GPa; hardness = ~60 GPa). However, a large bulk modulus only indicates that a material has low compressibility, which does not necessarily translate into a high value of strength since the latter is determined by its resistance against inelastic (large) structural deformations. To study the mechanical properties of OsB<sub>2</sub> under large structural deformations and understand how the distribution of the interstitial boron atoms affects its strength, we report in this communication first-principles calculations of ideal tensile and shear strength of OsB<sub>2</sub>. Density functional theory calculations of ideal strength, which is defined as the peak stress in the stress–strain curve in the weakest tensile stretch or shear slip direction, have been developed in recent years to determine the critical stress at which a perfect lattice becomes unstable under (tensile or shear) deformation strain.<sup>14–20</sup> It provides an assessment of the upper limit of the material strength that can be directly compared to nanoindentation measurements<sup>18</sup> and is more accurate in predicting material strengths than the conventional criteria of elastic constants such as bulk and shear moduli obtained at the equilibrium structure. This is because ideal strength calculations examine the stress–strain relation at large structural deformation and, therefore, can reveal any potential structural softening due to bond-charge redistribution

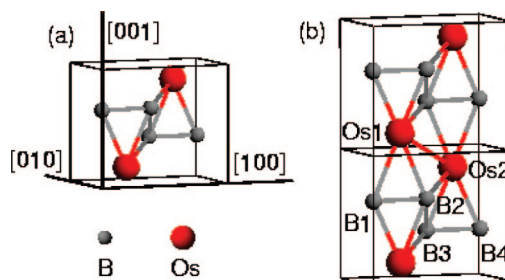


**Figure 1.** (a) The conventional unit cell of OsB<sub>2</sub>. (b) The 1 × 1 × 2 super cell showing the Os–Os layer that is strong against shear deformation in the [100] direction but weak in the [010] direction.

under strain. Our calculations show that, although its ideal tensile strength is higher than 20 GPa, the ideal shear strength of OsB<sub>2</sub> is only 9.1 GPa, barely higher than that of pure iron (7.2 GPa).<sup>19</sup> An examination of the atomistic structure shows that, while the interstitial boron atoms enhance the strength of OsB<sub>2</sub> by forming strong, directional covalent bonds with most of the Os atoms, there remain Os–Os metallic bonding layers which are deformed easily by shear stresses in certain directions, despite the high composition ratio of boron in OsB<sub>2</sub>. These weak Os–Os layers reduce greatly the resistance of OsB<sub>2</sub> against large shear deformations in these easy-slip directions.

In Figure 1, we show the orthorhombic unit cell of OsB<sub>2</sub> (Figure 1a), commonly used in previous calculations for its bulk modulus and electronic band structure, and a 1 × 1 × 2 supercell highlighting the weak (001) Os–Os layer, formed by the Os1 and Os2 atoms in the adjacent unit cells (Figure 1b). The triangular structure B1–Os1–B2 (or B3–Os2–B4) in the unit cell strengthens this Os–Os layer against the shear deformation in the [100] direction; however, in the [010] direction, the Os–Os layer is weak under the shear stress because most of the B–Os bonds are either perpendicular to this direction or lying outside of this Os–Os layer.

The calculated tensile stresses in various symmetric crystallographic directions are presented in Figure 2 (for calculation details, see the Supporting Information). The results identify the lowest peak stress (i.e., the ideal tensile strength) of 25.9 GPa in the [011] direction; this is much larger than the ideal tensile strength of pure iron (12.6 GPa).<sup>19</sup> The covalent B–Os bonds enhance the resistance of OsB<sub>2</sub> to tensile deformations in all these directions.

Figure 3 shows calculated shear stresses in the (001) plane along three high-symmetry directions. The lowest peak stress (i.e., the ideal shear strength) is 9.1 GPa in the (001)[010] shear direction, while the peak stress in the (001)[100] direction is nearly three times as large at 26.9 GPa. The highly anisotropic strength on the (001) plane is consistent with the structural analysis of the Os–Os layer in Figure 1, where B–Os–B triangles only enhance the resistance of the Os–Os layer against shear deformations in the (001)[100] shear direction. The shear strength of the Os–Os layer exhibits a ductile stretch pattern in the (001)[010] direction typical

<sup>†</sup> Shanghai Jiao Tong University.

<sup>‡</sup> University of Nevada, Las Vegas.

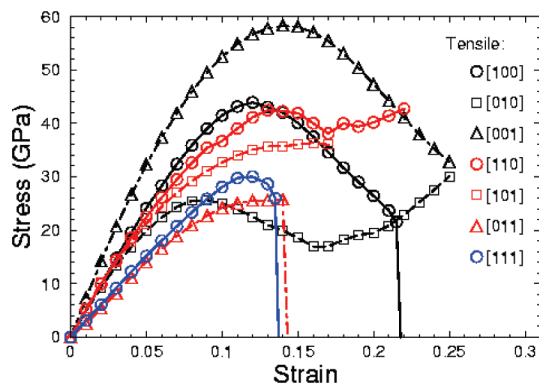


**Figure 2.** Calculated tensile stresses under the indicated tensile strains in different high-symmetry directions.

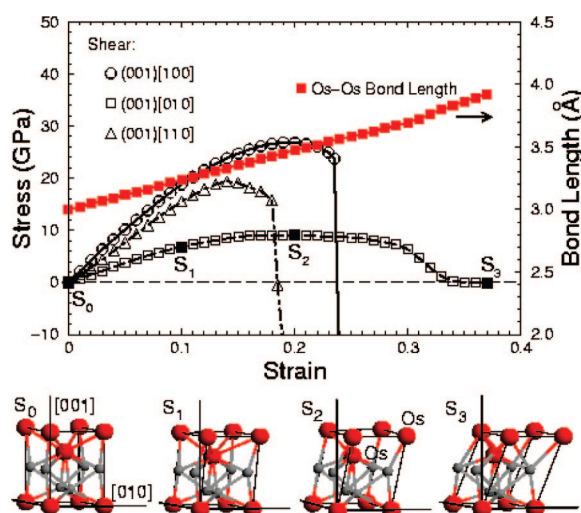


**Figure 3.** Calculated shear stresses and selected Os–Os bond length under indicated shear strains. Selected snapshots are shown for the structural deformation along the weakest (001)[010] shear direction. The symmetric unit cell of orthorhombic OsB<sub>2</sub> used in this figure is defined in the Supporting Information.

of metallic materials, while in the (001)[100] direction, it shows a brittle manner typical for super-hard materials. The structural deformation snapshots clearly show the bond breaking process in the Os–Os layer under the (001)[010] shear strains. The strong, directional covalent B–Os bonds normal to or lying outside of the (001) Os–Os layers do not help enhance the resistance against the large shear deformation in the (001)[010] shear direction.

Our calculated results can be reconciled with the high Vickers hardness<sup>3</sup> by examining the bonding anisotropy in the Os–Os (001) layer in orthorhombic OsB<sub>2</sub>: while the B–Os–B triangles make it difficult to shear break in the (001)[100] direction, shear deformation can easily occur in the (001)[010] direction. Since the indenter produces imprint by shear deforming in both the [100] and [010] directions on the (001) plane, the stronger resistance in the [100] direction plays a dominant role, giving rise to a high Vickers hardness, despite the weak shear strength in the [010] direction. The peak stress of 26.9 GPa in the (001)[100] shear direction agrees well with the measured Vickers hardness of 30 GPa on the (001) plane.<sup>3</sup> The high scratching hardness of OsB<sub>2</sub> (>20 GPa)<sup>1</sup> also can

be explained since OsB<sub>2</sub> powder contains microcrystals with different orientations and those with high shear strength can readily scratch the sapphire window. It should be noted that previous theoretical hardness estimates<sup>6,21</sup> give only an average hardness since they do not distinguish the crystal orientations of planes on which the hardness is measured. Our calculations reveal substantial disparity in shear strength along different directions in the easy-slip plane, indicating that OsB<sub>2</sub> is a very special example that has high (Vickers) hardness (>30 GPa) on the (001) plane but low shear strength (<10 GPa) on the same plane in the [010] direction. It suggests that ultra-hard materials identified by conventional hardness tests may have subtle weakness under certain shear loading conditions.

In summary, our ideal strength calculations show that, despite the high compositional ratio of boron in OsB<sub>2</sub> that enhances its tensile strength, highly anisotropic Os–Os (001) layers containing no B–Os and B–B bonds make it susceptible to failure in certain direction under moderate shear stresses. The ideal shear strength of OsB<sub>2</sub> is just 9.1 GPa, only slightly higher than that of pure iron (7.2 GPa),<sup>19</sup> rendering it unsuitable for originally proposed applications.<sup>1</sup> It highlights the importance of exploring atomistic deformation modes under various loading conditions in designing new ultra-hard materials.

**Acknowledgment.** Work supported by DOE Grant DE-FC52-06NA27684 and NNSF of China Grants 10574089 and 50532020.

**Supporting Information Available:** Details of ideal strength calculations, calculated structural parameters and elastic constants of OsB<sub>2</sub> compared with previous results, definition of a high symmetric OsB<sub>2</sub> unit cell, and calculated shear stress on the (011) plane along high-symmetry directions. This material is available free of charge via the Internet at <http://pubs.acs.org>.

## References

- (1) Cumberland, R. W.; Weinberger, M. B.; Gilman, J. J.; Clark, S. M.; Tolbert, S. H.; Kaner, R. B. *J. Am. Chem. Soc.* **2005**, *127*, 7264.
- (2) Kaner, R. B.; Gilman, J. J.; Tolbert, S. H. *Science* **2005**, *308*, 1268.
- (3) Hebbache, M.; Stuparevic, L.; Zivkovic, D. *Solid State Commun.* **2006**, *139*, 227.
- (4) Young, A. F.; Sanloup, C.; Gregoryanz, E.; Scandolo, S.; Hemley, R. J.; Mao, H. K. *Phys. Rev. Lett.* **2006**, *96*, 155501.
- (5) Chung, H. Y.; Weinberger, M. B.; Levine, J. B.; Kavner, A.; Yang, J. M.; Tolbert, S. H.; Kaner, R. B. *Science* **2007**, *316*, 436.
- (6) Gou, H. Y.; Hou, L.; Zhang, J. W.; Li, H.; Sun, G. F.; Gao, F. M. *Appl. Phys. Lett.* **2006**, *88*, 221904.
- (7) Chen, Z. Y.; Xiang, H. J.; Yang, J. L.; Hou, J. G.; Zhu, Q. S. *Phys. Rev. B* **2006**, *74*, 012102.
- (8) Chiodo, S.; Gotsis, H. J.; Russo, N.; Sicilia, E. *Chem. Phys. Lett.* **2006**, *425*, 311.
- (9) Hao, X. F.; Wu, Z. J.; Xu, Y. H.; Zhou, D. F.; Liu, X. J.; Meng, J. J. *Phys.: Condens. Matter* **2007**, *19*, 196212.
- (10) Wang, Y. X. *Appl. Phys. Lett.* **2007**, *91*, 101904.
- (11) Zhang, R. F.; Veprek, S.; Argon, A. S. *Appl. Phys. Lett.* **2007**, *91*, 201914.
- (12) Fan, C. Z.; Zeng, S. Y.; Li, L. X.; Zhan, Z. J.; Liu, R. P.; Wang, W. K.; Zhang, P.; Yao, Y. G. *Phys. Rev. B* **2006**, *74*, 125118.
- (13) Zheng, J. C. *Phys. Rev. B* **2005**, *72*, 052105.
- (14) Telling, R. H.; Pickard, C. J.; Payne, M. C.; Field, J. E. *Phys. Rev. Lett.* **2000**, *84*, 5160.
- (15) Chacham, H.; Kleinman, L. *Phys. Rev. Lett.* **2000**, *85*, 4904.
- (16) Jhi, S. H.; Louie, S. G.; Cohen, M. L.; Morris, J. W., Jr. *Phys. Rev. Lett.* **2001**, *87*, 075503.
- (17) Ogata, S.; Li, J.; Yip, S. *Science* **2002**, *298*, 807.
- (18) Krenn, C. R.; Roundy, D.; Cohen, M. L.; Chrzan, D. C.; Morris, J. W., Jr. *Phys. Rev. B* **2002**, *65*, 134111.
- (19) Clatterbuck, D. M.; Chrzan, D. C.; Morris, J. W. *Acta Mater.* **2003**, *51*, 2271.
- (20) Zhang, Y.; Sun, H.; Chen, C. F. *Phys. Rev. Lett.* **2004**, *93*, 195504; *Phys. Rev. Lett.* **2005**, *94*, 145505.
- (21) Simunek, A. *Phys. Rev. B* **2007**, *75*, 172108.

JA801520V